ELSEVIER

Journal of Materials Processing Technology 124 (2002) 319–328

Journal of Materials Processing Technology

www.elsevier.com/locate/jmatprotec

Sensitivity based optimization of sheet metal forming tools

Włodzimierz Sosnowski*, Izabela Marczewska, Artur Marczewski

Institute of Fundamental Technological Research, Polish Academy of Sciences, Świętokrzyska 21, 00-049 Warsaw, Poland

Received 7 March 2000; received in revised form 19 March 2002; accepted 15 April 2002

Abstract

The shape of the first of two contacting bodies is optimized on the basis of sensitivities calculated for the second body, i.e. workpiece. The finite element simulation of sheet metal forming process and direct differentiation method of sensitivity analysis are used. Some energy measures of deforming sheet metal treated as a cost functional and its gradients with respect to the tool (punch) shape parameters is evaluated. Tool shape optimization based on "exact" sensitivity results is performed. Calculated sensitivities with respect to the tool shape parameters are the input for each iteration of the optimization algorithm (treated here as a "black box") from which new values of the design variables are obtained until the cost functional is minimized, yielding the optimal shape for the considered functional.

As an example the axisymmetrical part of the compressor cover produced in one of sheet stamping factories is considered. It was impossible to produce it without shape modifications. Energy consumption measure is minimized here but other objective functions can easily be included in the algorithm.

Keywords: Sheet metal forming; Sensitivity; Optimization; Tools design

1. Introduction

The subject of this paper is the shape and nonshape 'exact sensitivity' based optimization of transient problems of sheet metal forming. In the last years the sensitivity analysis has been found the most effective (exact, reliable and computationally efficient) tool in optimal design.

Finite element simulation of industrial sheet metal forming processes is now widely used in design, in the automotive industry for instance. The spring-back, wrinkling and fracture phenomena can be simulated, as was written for instance almost 10 years ago in the first authors paper [11] published in the Journal of Materials Processing Technology and in many other papers related to the finite element simulation of sheet metal forming processes. Tool shape optimization is still performed, however, by classical trial and error numerical experiments and/or appropriate adjustments in stamping factories.

Classical mathematical methods of optimization based on sensitivity analysis have been developed and applied mainly in structural engineering. A short state of art in this field and interesting sensitivity based shape optimization of heat conduction systems are presented in [1]. Application of these methods in the area of metal forming appears to be limited to stationary problems [3]. For effective optimization of frictional contact problems with unilateral constraints directional derivatives should be considered [5].

The analytical (exact) calculations of sensitivities of the problem functions with respect to the design parameters are relatively complex, which is the reason that the majority of known solutions are based on the finite difference sensitivity techniques [6,12].

Possible gains can be achieved during the process by minimization of forming energy consumption, tool wear, number of operations, friction forces or maximization of admissible tool velocity. Also the better product quality can be expected with proper surface characteristics (without wrinkling or other geometrical defects), uniform blank thickness, strain and stress distribution, smaller residual stresses etc.

In sheet metal forming various and sometimes contradictory criteria must be satisfied, so many different objective functions are necessary in order to obtain proper quality and product cost. Very often traditional trial and error procedures should be used as complementary to minimization procedures. Possible design variables are initial sheet thickness, blankholder forces, drawbed profiles and location, friction law coefficients and parameters defining tool shape. The choice of objective function in optimization problem is not unique. It depends on these features of the final product, which are most important for the producers. Number of

* Corresponding author.
E-mail address: wsosn@ippt.gov.pl (W. Sosnowski).

0924-0136/02/$ – see front matter © 2002 Elsevier Science B.V. All rights reserved.
PII: S0924-0136(02)00220-0

possible objective functions which can be applied in metal forming are listed and discussed in [4].

In this paper the minimization of some measure of the global dissipation energy is performed

$$\Psi = \int_{\Omega}\int_{0}^{t^e} (\boldsymbol{\sigma}^{\mathrm{T}}\dot{\varepsilon})\,\mathrm{d}\Omega\,\mathrm{d}t \tag{1}$$

The region occupied by the body W varies in time t, t^e is the time at the end of deformation process. The stress and strain rate fields are denoted by σ and $\dot{\varepsilon}$, respectively. The expression (1) must be calculated for the whole deformation process by accumulation of all incremental values. Sometimes we must admit more than one objective function to be considered simultaneously, so many functions can be used at the same time for the multicriterion optimization.

After calculation of sensitivity gradients $\mathrm{d}\Psi/\mathrm{d}h_i$ of the objective function $\Psi(h_i)$ with respect to the design parameters vector $\mathbf{h} = \{h_1, \ldots, h_n\}$ at the end of the process (which is crucial for time dependent plasticity problems) the minimization of the function (1) with respect to the design parameter $\mathbf{h}$ must be performed. Next the design variable must be updated and all calculations are followed by the next step of the iterative optimization procedure. It means that it is necessary to repeat the calculations of the whole deformation process in order to get the new values of the function Ψ, its gradients and problem constraints. So the optimization procedure is relatively expensive as the number of optimization iterations is equal to the number of numerical simulation of the sheet metal forming process, including necessary sensitivity calculations with respect to the basic design variables during all these simulations. More details about this algorithm and constraints are given in Section 4.

In this paper exact sensitivities are obtained by direct differentiation of all functions entering the problem and included into the flow approach-based nonlinear code for finite element simulation of sheet metal forming.

As an example the axisymmetrical part of the compressor cover produced in one of sheet stamping factories is considered. For the time being only total strain energy consumption is minimized but any other objective function can easily be included into the algorithm.

The design variable vector $\mathbf{h}$ is assumed to depend on the tool shape. Tool master nodes with coordinates X which participate in design variation are specified. An useful way to do this is to represent tool surface as polynomials or splines and calculate sensitivities with respect to its coefficients. The proper choice of tool surface representation and design variable selection are shortly discussed in Section 5.1.

2. Basic formulation of sheet metal forming

The flow approach to metal forming problems with the rigid–viscoplastic material model is used as the basis in this paper [7,14].

The virtual work expression (equilibrium equation in the weak form) to be solved reads

$$\int_{\Omega} \sigma^{\mathrm{T}}\boldsymbol{\delta}\dot{\varepsilon}\,\mathrm{d}\Omega = \int_{\Omega}\mathbf{f}^{\mathrm{T}}\delta\mathbf{v}\,\mathrm{d}\Omega + \int_{\partial\Omega}\mathbf{t}^{\mathrm{T}}\delta\mathbf{v}\,\mathrm{d}(\partial\Omega) \tag{2}$$

where $\mathbf{v}$ denotes the velocity field, $\mathbf{f}$ the distributed volumetric load, $\mathbf{t}$ the traction on the boundary and integrals are taken over the actual body volume element $\mathrm{d}\Omega$ or its surface element $\mathrm{d}(\partial\Omega)$, respectively.

Stresses are calculated from the constitutive equation

$$\sigma_{ij} = s_{ij} + p\delta_{ij} \tag{3}$$

$$s_{ij} = 2\mu^*\dot{\varepsilon}_{ij} \tag{4}$$

where s_{ij} is the Cauchy stress deviator, p denotes the mean stress and δ_{ij} the Kronecker delta. The constitutive function μ^* is defined in the flow problem as [14]

$$\mu^* = \frac{\bar{\sigma}}{3\dot{\bar{\varepsilon}}} = \frac{\sigma_y + (\dot{\bar{\varepsilon}}/\gamma)^{1/n}}{3\dot{\bar{\varepsilon}}} \tag{5}$$

Here, σ_y is the current static uniaxial tensile yield stress of the material, $\bar{\sigma}$ the equivalent stress

$$\bar{\sigma} = \left(\tfrac{3}{2}s_{ij}s_{ij}\right)^{1/2} \tag{6}$$

where $\dot{\bar{\varepsilon}}$ is the effective inelastic strain rate

$$\dot{\bar{\varepsilon}} = \left(\tfrac{2}{3}\dot{\varepsilon}_{ij}\dot{\varepsilon}_{ij}\right)^{1/2} \tag{7}$$

and γ, n are physical parameters of the rigid–viscoplastic model used.

For pure plasticity assumed later in this paper we set $\gamma \to \infty$ and Eq. (5) yields simply

$$\mu^* = \frac{\sigma_y}{3\dot{\bar{\varepsilon}}} \tag{8}$$

For strain hardening plastic materials the yield limit σ_y is a function of the effective inelastic strain $\bar{\varepsilon}$

$$\sigma_y = \sigma_y(\bar{\varepsilon}) \tag{9}$$

where $\bar{\varepsilon}$ has to be computed as the time integral of $\dot{\bar{\varepsilon}}$.

The analogy between plastic flow and incompressible elasticity allows the treatment of pure plastic flow problem using a numerical code developed for linear elasticity. The incompressibility condition must be satisfied.

In sheet metal forming the shell theory as the simplification of 3D problems is used and large plastic deformations of thin sheets of metal are treated as elastic incompressible shell deformations. Plane stress assumptions are used in shell theory so the incompressibility can be easily achieved by adjusting the shell thickness during consecutive steps of the solution to ensure the constant volume.

After spatial finite element discretization the ‘secant’ stiffness matrix $\mathbf{K}$ depends on the nodal velocities $\dot{\mathbf{q}}$ through the parameter μ^* so that an iterative process is needed to find the solution vector $\dot{\mathbf{q}}$

$$\mathbf{K}^{(i)}\dot{\mathbf{q}}^{(i+1)} = \mathbf{Q}, \qquad i = 0, 1, 2, \ldots \tag{10}$$

in which $\mathbf{Q}$ denotes the external force and

$$\mathbf{K}^{(i)} = \mathbf{K}[\mu^*(\dot{\mathbf{q}}^{(i)})] \tag{11}$$

The element contributions to the stiffness matrix $\mathbf{K}$ and the nodal forces vector $\mathbf{Q}$ are

$$\mathbf{K}_{(ij)} = 2\pi \int_l \mathbf{B}_i^{\mathrm{T}} \mathbf{D} \mathbf{B}_j r \, \mathrm{d}s \tag{12}$$

$$\mathbf{Q}_{(i)} = 2\pi \int_l \mathbf{N}_i \mathbf{t} r \, \mathrm{d}s + 2\pi r_i \mathbf{p}_i \tag{13}$$

where l is the element length, r the radial distance from the symmetry axis, and $\mathbf{t}$ and $\mathbf{p}$ are the surface and point load vectors, respectively. Details of the generalized strain rate–velocity relationships for the axisymmetric viscous shell are given in Appendix A and in paper [7].

Please, note that in this approach $\mathbf{K}^{(i)}$ is not the function of $\mathbf{q}$ because $\mathbf{q}$ is not the main unknown, $\mathbf{q}$ is calculated for a rigid–plastic material as the product of velocity $\dot{\mathbf{q}}$ and pseudo-time increment.

Using the Newton–Raphson scheme the ith residual is defined as

$$\mathbf{R}^{(i)} = \mathbf{Q} - \mathbf{K}^{(i)} \dot{\mathbf{q}}^{(i)} \tag{14}$$

while the iterative correction $\delta\dot{\mathbf{q}}^{(i)}$ such that

$$\dot{\mathbf{q}}^{(i+1)} = \dot{\mathbf{q}}^{(i)} + \delta\dot{\mathbf{q}}^{(i)}, \qquad i = 0, 1, 2, \ldots \tag{15}$$

is computed from

$$\mathbf{K}_{\mathrm{T}}^{(i)} \delta\dot{\mathbf{q}}^{(i)} = \mathbf{R}^{(i)} - \frac{\partial \mathbf{K}}{\partial \dot{\mathbf{q}}} \dot{\mathbf{q}} \tag{16}$$

where

$$\mathbf{K}_{\mathrm{T}} = \mathbf{K} + \frac{\partial \mathbf{K}}{\partial \mu^*} \frac{\partial \mu^*}{\partial \dot{\mathbf{q}}} \dot{\mathbf{q}} \tag{17}$$

is the tangent stiffness matrix.

3. Tool shape sensitivity in sheet metal forming

For the design of the new sheet metal forming process it is useful to know the sensitivities of many different functions describing stress, strain, plastic strain, thickness distribution inside deformed blank with respect to the shape parameters of the tools (punch, die, blankholder). If the shape parameter changes are not large, the first gradient of the function with respect to shape parameter can be treated as the proper sensitivity measure.

In paper [10] direct differentiation method (DDM) was used in order to calculate thickness sensitivity with respect to friction. The extension of this algorithm to the shape sensitivity is based on domain parametrization (control volumes) approach (DPA) [3].

The response functional (1) must be mapped to the reference configuration

$$x = x(\xi, h)$$

using the determinant J of the Jacobian matrix

$$(\mathbf{J})_{ij} = \frac{\partial x_i}{\partial \xi_j} \tag{18}$$

Typical for many standard finite element codes isoparametric element concept was used in this mapping.

The Eq. (2) in the reference configuration are as follows:

$$\int_{\Omega_0} (\sigma^{\mathrm{T}} \delta\dot{\varepsilon} - \mathbf{f}^{\mathrm{T}} \delta\mathbf{v}) J \, \mathrm{d}\Omega_0 - \int_{\partial\Omega_0} \mathbf{t}^{\mathrm{T}} \delta\mathbf{v} \partial J \, \mathrm{d}(\partial\Omega_0) = 0 \tag{19}$$

where ∂J defines the surface transformation into the reference configuration, $\partial J = J[\mathbf{J}^{-\mathrm{T}}\mathbf{n}]$ and $\mathbf{n}$ is the normal vector field in the current configuration.

3.1. Sensitivity of velocity fields

The gradients of velocity field with respect to shape parameter $\mathbf{h}$ can be calculated after linearization of (19) as follows:

$$\begin{aligned} \mathbf{K}_{\mathrm{T}} \frac{\mathrm{d}\dot{\mathbf{q}}}{\mathrm{d}\mathbf{h}} = &- \int_{\Omega_0} 2\mathbf{B}^{\mathrm{T}} \left(\frac{\mathrm{d}\mu^*}{\mathrm{d}\mathbf{h}} \mathbf{B} + \mu^* \frac{\mathrm{d}\mathbf{B}}{\mathrm{d}\mathbf{h}} \right) \dot{\mathbf{q}} J \, \mathrm{d}\Omega_0 \\ &- \int_{\Omega_0} 2\mu^* \left(\frac{\mathrm{d}\mathbf{B}}{\mathrm{d}\mathbf{h}} \right)^{\mathrm{T}} \mathbf{B}\dot{\mathbf{q}} J \, \mathrm{d}\Omega_0 - \int_{\Omega_0} 2\mu^* \mathbf{B}^{\mathrm{T}} \mathbf{B}\dot{\mathbf{q}} \frac{\mathrm{d}J}{\mathrm{d}\mathbf{h}} \mathrm{d}\Omega_0 \\ &- \int_{\Omega_0} \left(\frac{\mathrm{d}\mathbf{B}}{\mathrm{d}\mathbf{h}} \right)^{\mathrm{T}} \mathbf{pI} J \, \mathrm{d}\Omega_0 - \int_{\Omega_0} \mathbf{B}^{\mathrm{T}} \mathbf{pI} \frac{\mathrm{d}\partial J}{\mathrm{d}\mathbf{h}} \mathrm{d}\Omega_0 \end{aligned} \tag{20}$$

where $\dot{\mathbf{q}}$ is a typical nodal velocity affected by the perturbation of the design variable $\mathbf{h}$, $\mathbf{B}$ the velocity–strain rate matrix, J the determinant of the Jacobian matrix, μ^* the viscosity. The matrix $\mathbf{B}$ and its derivatives with respect to two independent design parameter sets selected as described in Section 5.1 are given in Appendix A.

In plasticity the effect of the pressure field $\mathbf{p}$ on velocity can be neglected, so the last two terms in Eq. (20) vanish and the sensitivity of the normal vector does not enter into such simplified model.

The right hand side of the above expression was calculated by direct differentiation (i.e. without finite difference scheme) coupled with control volume approach which is relatively easy to implement because of its full analogy to isoparametric element concept. Errors typical for semianalytical finite difference methods are avoided. We can observe that on the left hand side of both equations, for both fundamental and sensitivity problems the same stiffness matrix appears. This fact makes the algorithm efficiency much higher.

The sensitivity of viscosity μ^* with respect to the design parameter can be calculated using the chain rule of differentiation, thus

$$\frac{\mathrm{d}\mu^*}{\mathrm{d}h_i} = \frac{\partial \mu^*}{\partial \dot{\mathbf{q}}} \frac{\mathrm{d}\dot{\mathbf{q}}}{\mathrm{d}h_i} \tag{21}$$

In fact the viscosity does not depend explicitly on displacements $\mathbf{q} = \dot{\mathbf{q}}\Delta t$

$$\frac{\partial \mu^*}{\partial \dot{\mathbf{q}}^{(i)}} = \frac{\partial \mu^*}{\partial \dot{\bar{\varepsilon}}} \frac{\partial \dot{\bar{\varepsilon}}}{\partial \dot{\varepsilon}} \frac{\partial \dot{\varepsilon}}{\partial \dot{\mathbf{q}}^{(i)}} \tag{22}$$

where from Eq. (5) we have

$$\frac{\partial \mu^*}{\partial \dot{\bar{\varepsilon}}} = \frac{[-\sigma_y + ((1/n) - 1)(\dot{\bar{\varepsilon}}/\gamma)^{1/n}]}{3\dot{\bar{\varepsilon}}^2} \tag{23}$$

$$\left(\frac{\partial \dot{\bar{\varepsilon}}}{\partial \dot{\varepsilon}}\right)_{1\times 6} = \frac{2\dot{\varepsilon}^{\mathrm{T}}}{3\dot{\bar{\varepsilon}}} = \frac{2\mathbf{B}^{\mathrm{T}}\dot{\mathbf{q}}^{\mathrm{T}}}{3\dot{\bar{\varepsilon}}} \tag{24}$$

$$\left(\frac{\mathrm{d}\dot{\varepsilon}}{\mathrm{d}\dot{\mathbf{q}}}\right)_{6\times N} = \frac{\mathrm{d}(\mathbf{B}\dot{\mathbf{q}})}{\mathrm{d}\dot{\mathbf{q}}} = \mathbf{B} \tag{25}$$

In Appendix A the derivatives of matrix $\mathbf{B}$ with respect to two independent design parameters sets chosen as described in Section 5.1 are given.

3.2. Sensitivities of the energy function with respect to the design parameters

Total strains are calculated incrementally during deformation process

$$\varepsilon^{t+\Delta t} = \varepsilon^t + \Delta\varepsilon^t \tag{26}$$

Strain increment $\Delta\varepsilon^t$ depends on strain rate and time increment

$$\Delta\varepsilon^t = \int_t^{t+\Delta t} \dot{\varepsilon}^t \,\mathrm{d}t \tag{27}$$

For typical stamping process and for relatively small time increments the Eq. (27) can be rewritten as follows:

$$\Delta\varepsilon^t = \dot{\varepsilon}^t \Delta t \tag{28}$$

The energy dissipation given by formula (1) has to be calculated incrementally

$$\Psi^{t+\Delta t} = \Psi^t + \Delta\Psi^t \tag{29}$$

where the energy dissipation increment $\Delta\Psi^t$ equals

$$\Delta\Psi^t = \sum_{e=1,\ldots,E} \int_{\Omega_e} (\sigma^t)^{\mathrm{T}} \Delta\varepsilon^t \,\mathrm{d}\Omega_e \tag{30}$$

where E is the number of finite elements in the system.

In practical applications some energy measure can be minimized yielding optimal design close to exact solution. In this paper such energy measure was calculated as the function of stress and strain fields calculated at the end of deformation process, $t = t^e$

$$\Psi^* = \sum_{e=1,\ldots,E} \int_{\Omega_e} (\sigma^{t^e})^{\mathrm{T}} \varepsilon^{t^e} \,\mathrm{d}\Omega_e \tag{31}$$

Let us consider the energy dissipation measure given by formula (31). Its derivation with respect to design variable h_j results in

$$\frac{\mathrm{d}\Psi^*}{\mathrm{d}h_j} = \left(\frac{(\mathrm{d}\sigma)^{\mathrm{T}}}{\mathrm{d}h_j}\varepsilon + \sigma^{\mathrm{T}}\frac{\mathrm{d}\varepsilon}{\mathrm{d}h_j}\right) \tag{32}$$

where to simplify notation the index t^e is dropped in all symbols related to the end of deformation process.

Strains are calculated as product of strain rates times pseudo-time increment Δt, so strain shape sensitivity equals

$$\frac{\mathrm{d}\varepsilon}{\mathrm{d}h_j} = \frac{\mathrm{d}\dot{\varepsilon}}{\mathrm{d}h_j}\Delta t \tag{33}$$

In case of rigid–plastic material model t is not the real time—the absence of viscosity allows to treat the time just as the integration parameter in nonlinear equations.

Strain rate derivative with respect to design variables is equal to

$$\frac{\mathrm{d}\dot{\varepsilon}^{(i+1)}}{\mathrm{d}h_j} = \frac{\mathrm{d}\mathbf{B}}{\mathrm{d}h_j}\dot{\mathbf{q}}^{(i+1)} + \mathbf{B}\frac{\mathrm{d}\dot{\mathbf{q}}^{(i)}}{\mathrm{d}h_j} \tag{34}$$

where i denotes the step counter.

The stress σ in flow approach depends on strain rate and on material tangent matrix $\mathbf{D}$ only

$$\sigma = \mathbf{D}(\boldsymbol{h}, \dot{\varepsilon})\dot{\varepsilon} \tag{35}$$

The stress shape sensitivity equals

$$\frac{\mathrm{d}\sigma}{\mathrm{d}h_j} = \frac{\mathrm{d}\mathbf{D}}{\mathrm{d}h_j}\dot{\varepsilon} + \mathbf{D}\frac{\mathrm{d}\dot{\varepsilon}}{\mathrm{d}h_j} \tag{36}$$

where $\mathbf{D}$ is material tangent matrix.

$$\frac{\mathrm{d}\mathbf{D}}{\mathrm{d}h_j}\dot{\varepsilon} = \frac{\partial \mathbf{D}}{\partial \dot{\varepsilon}}\frac{\mathrm{d}\dot{\varepsilon}}{\mathrm{d}h_j}\dot{\varepsilon} + \frac{\partial \mathbf{D}}{\partial h_j}\dot{\varepsilon} \tag{37}$$

$$\frac{\mathrm{d}\sigma}{\mathrm{d}h_j} = \left[\frac{\partial \mathbf{D}}{\partial \dot{\varepsilon}}\dot{\varepsilon} + \mathbf{D}\right]\left(\frac{\mathrm{d}\mathbf{B}}{\mathrm{d}h_j}\dot{\mathbf{q}}^{(i+1)} + \mathbf{B}\frac{\mathrm{d}\dot{\mathbf{q}}^{(i)}}{\mathrm{d}h_j}\right) + \frac{\partial \mathbf{D}}{\partial h_j}\dot{\varepsilon} \tag{38}$$

Exact calculation of $\mathrm{d}\mathbf{D}/\mathrm{d}h_j$ involves thickness differentiation with respect to h_j which can be performed similarly as it was done in paper [10] where thickness sensitivity with respect to friction was established.

Some authors [9] have proposed for above calculations some simplifications. They neglect $\mathbf{D}$ matrix derivatives in Eq. (38) assuming they are small

$$\frac{\mathrm{d}\sigma^{(i+1)}}{\mathrm{d}h_j} = \frac{\mathrm{d}\sigma}{\mathrm{d}\dot{\varepsilon}}\frac{\mathrm{d}\dot{\varepsilon}}{\mathrm{d}h_j} = \mathbf{D}\left(\frac{\mathrm{d}\mathbf{B}}{\mathrm{d}h_j}\dot{\mathbf{q}}^{(i+1)} + \mathbf{B}\frac{\mathrm{d}\dot{\mathbf{q}}^{(i)}}{\mathrm{d}h_j}\right) \tag{39}$$

Above equation can be applied when thickness distribution is not of primary concern in shape optimization. Sensitivities given by Eq. (32) can be used directly in optimization algorithm.

3.3. Design elements and master nodes

The derivative of any function, for instance $\mathbf{B}(x)$ with respect to the design variable can be calculated using the chain rule of differentiation, where simplified dependency of any node coordinate on the master node coordinate can be assumed for a specific problem at hand.

For the tool shape sensitivity such dependency must be established for active sets of nodes with coordinates x being in full contact with the part of the tool, where master nodes with coordinates X are defined. For these active nodes the derivative of $\mathbf{B}(x)$ with respect to the design variable h_k is equal to

$$\frac{\partial \mathbf{B}}{\partial h_k} = \frac{\partial \mathbf{B}}{\partial x_i}\frac{\partial x_i}{\partial X_j}\frac{\partial X_j}{\partial h_k} \tag{40}$$

when some specific master node coordinate is chosen as the design parameter $\mathbf{h} = X_3$, as was assumed for one of design parameters set in numerical example presented in Section 5, the above equation simplifies to

$$\frac{\partial \mathbf{B}}{\partial X_3} = \frac{\partial \mathbf{B}}{\partial x_i}\frac{\partial x_i}{\partial X_3} \tag{41}$$

4. Optimization algorithm

Shape sensitivities can be used directly in optimization using the sequential quadratic programming algorithm which was treated as a ''black box'', so details about it are not given in this paper but can be found in [8]. General scheme of calculations is shortly described in next section where numerical example is presented.

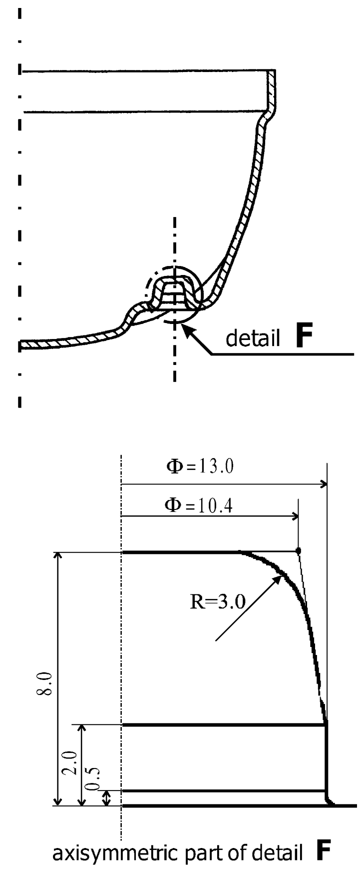

Fig. 1. Compressor cover produced by stamping factory HYDRAL. Dimensions are given in millimeter.

5. Numerical example

An axisymmetric part of a compressor cover produced by the stamping factory HYDRAL in Wroclaw (Poland) shown as a detail marked by letter F in Fig. 1 is considered. The diameter of this axisymmetric detail is denoted by ϕ and R denotes rounding. Some of dimensions, for instance the diameter $\phi = 13$ mm or detail height 8 mm are fixed (cannot be changed during optimization), some defining upper part shape of this detail are free do design. The deep drawing of this detail was impossible at the beginning of production, due to the localization effects (failures near the bottom part of the workpiece or excessive thinning of the blank sheet) so some optimization of tool shape by simple numerical simulation and trial and error procedure was undertaken first [2] and checked next against optimal solutions obtained with finite difference sensitivities.

Now we will try to do it in a more advanced manner, by exact shape sensitivity calculations and optimization by using the sequential quadratic programming method [8].

5.1. Design variable selection

The possible punch geometry representation could be expressed in terms of line segments or spline functions but the relatively large number of design variables would be needed for smooth punch surface description in the first case and wavy contour could be expected in the other case [6].

So the best choice is performed when optimized part of the punch shape is described by polynomials. In this paper the simple parabolas are taken with some design constraints imposed on their coefficients and limiting points 1 and 2 (see Fig. 2). Such boundary representation assures smoothness of the punch surface and gives possibility to reduce the number of design variables just to three polynomial coefficients, or even to one radial coordinate of the parabola inner point 3.

The shape sensitivities are calculated analytically by DDM with respect to two independent design variables sets:

- In first case vector $\mathbf{h}$ contains only three components namely, the parabola parameters a, b and c. Each consecutive approximation of this vector defines a new punch shape.
- In second case only one radial coordinate of the parabola's inner point 3 is chosen as the design variable $\mathbf{h} = X_3$.

The solutions are compared with results obtained by the same optimization method but different sensitivity calculations that is by the finite difference method.

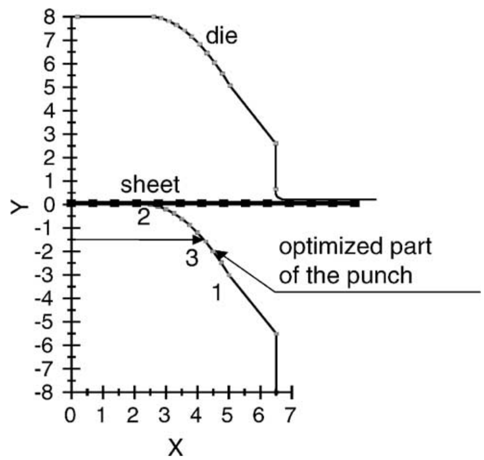

Fig. 2. Initial tools shape. Optimized part of the punch denoted by thick line.

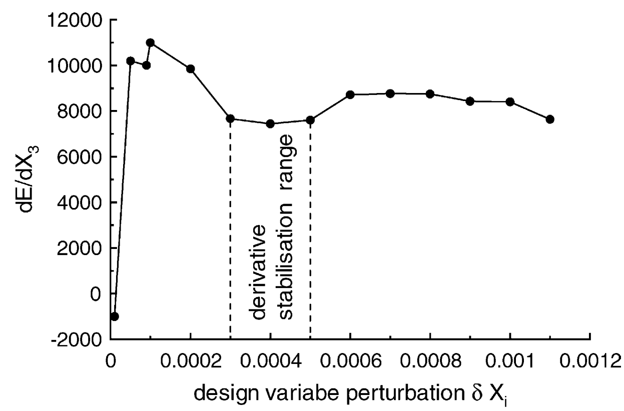

Fig. 3. Design variable perturbation choice for finite difference sensitivity calculations.

In order to calculate the sensitivities of energy function by finite difference method, the proper perturbation of design variable must be established. In Fig. 3 the results of such analysis for different perturbations of radial coordinate X_3 of the parabola inner point 3 is shown. The value of 0.0004 was chosen as some approximation of the optimal perturbation.

5.2. Summary of the algorithm in this specific example

1. Start optimization program with initial parabolic part of the punch described by parabola $\mathbf{h} = (a_0, b_0, c_0)$ or $\mathbf{h} = X_3$.
2. Calculate strain energy measure and its gradients with respect to the vector **h**.
3. Minimize energy by calculating its new value and new parabolic shape **h**.
4. Compute new punch shape and repeat steps 2 and 3.
5. End if in two consecutive steps energy value does not differ from the previous value more than assumed tolerance.

The solutions will be compared with results obtained by the same optimization method but different sensitivities calculations—by finite difference method.

5.3. Results

In Fig. 4 the optimization path in the design space obtained with sequential programming algorithm described shortly in the paper is shown. The minimal energy measure of 478.2521 N m was calculated by finite element code MARC and corresponds to the design variable value of $X_3 = 3.9892$ mm. This value defines the parabola $y = -0.19069x^2 + 0.230245x + 0.6163$ which describes optimal punch part shape designed, see Fig. 5.

Almost the same parabola was obtained when sensitivities were calculated by the DDM as shown in Fig. 5. The calculated energy consumption was significantly smaller in this case (it was equal to 392.16 N m). Also the shape obtained with the second set of design parameters, i.e. with parabola inner point variation was almost identical. The

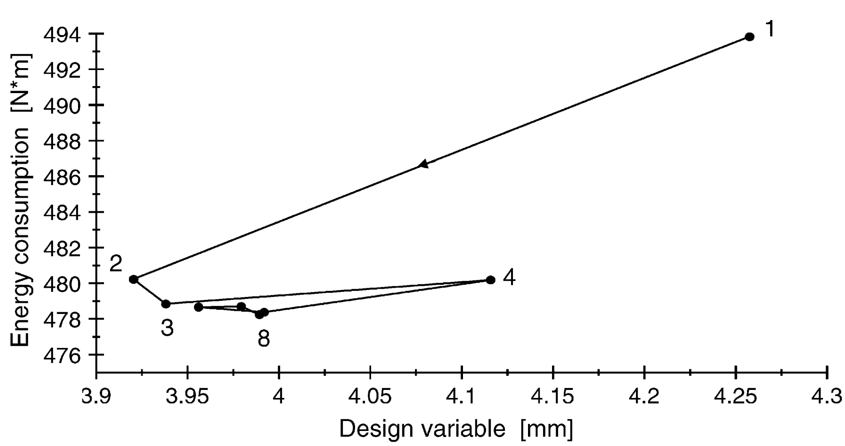

Fig. 4. Optimization path in the design space with sequential programming algorithm. Energy calculated by program MARC.

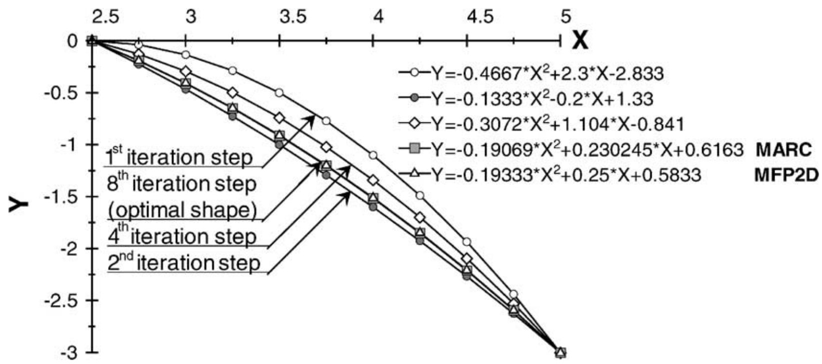

Fig. 5. HYDRAL test. Intermediate and optimal shapes of the optimized part of the punch.

calculations were about two times longer in the latter case however. The whole analysis was completed by some trial and error punch travel and die shape adjustment.

To our opinion the new methods of the tool shape optimization should be confirmed with other, more appropriate objective function. For the time being only the simplest energy consumption function was chosen. After reading some referee comments authors decided to include additional checking calculations of this energy consumption function by the 3D version of our simulation code.

Values of energy were checked by 3D code for eight cases of different values of design variable X_3. Comparison of results obtained for 2D axisymmetric case, and 3D planar strain case is shown in Fig. 6. On horizontal axis there are the values of design variable X_3 and on vertical axis there are the values of energy. It is observed that the 2D curve of energy is smoother than the one obtained by 3D calculations. The values of energy are similar, the small discrepancies are due to the different 2D and 3D discrete compressor cover part discretization. In both cases the minimal values of energy correspond to the optimal value of design parameter $X_3 = 3.9892$ mm. The deformed shapes of the blank for different punch travels and collapse zone developed are shown in Fig. 7.

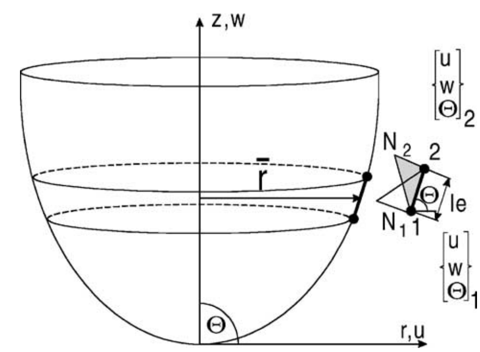

Fig. 6. Nodal displacements vectors and geometry description for 2-node, 2D axisymmetrical element.

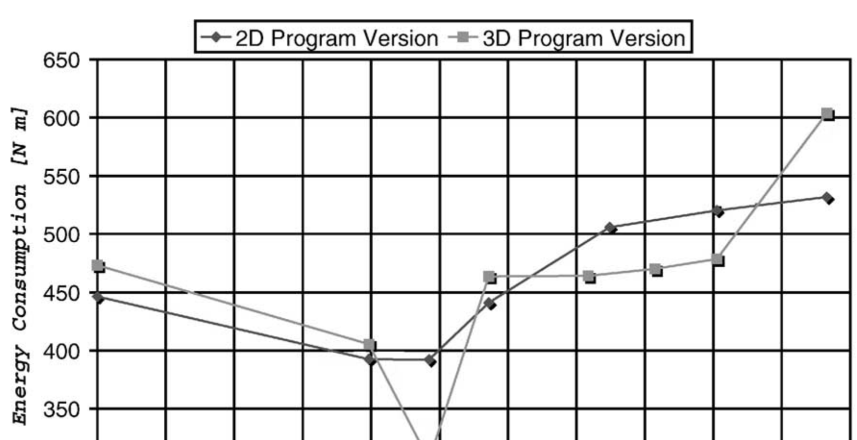

Fig. 7. Comparison of energy consumption curves calculated by 2D and 3D programs.

6. Conclusions

1. The parameter and shape optimization algorithm applied in practice may substantially reduce production costs in industrial sheet metal forming.
2. Sensitivity gradient evaluation based on strict analytical solutions are the most difficult task which has to be done in order to solve specific problems at hand. For effective optimization of frictional contact problems with unilateral constraints the directional derivatives should be considered.
3. In practical applications the proposed simple functions (parabolas) describing optimized shape of tool parts must be replaced by more general functions, for instance special polynomials or splines.
4. The choice of proper objective function is decisive for the optimization results. It is relatively easy to include any objective function. The punch shape corresponding to the minimal dissipation reduces the probability of local sheet failure. Similar or better effects can be achieved by introducing such objective functions as maximal local energy rate or maximum effective strain rate.
5. The selection of the optimization algorithm may be crucial for the effectiveness of the procedure. The tests presented using the sequential quadratic programming method shows its dependence of efficiency on the class of the objective functions.

Acknowledgements

We would like to acknowledge the work of Prof. C. Agelet de Saracibar Bosh from CIMNE Barcelona who wrote the program MFP2D used after some extension in this paper. Also the financial support of the Polish Committee for Scientific Research, grant 7T08B03612 is appreciated.

Appendix A

Strain rate to velocity matrix $\mathbf{B}_i$

$$\mathbf{B}_i = \begin{bmatrix} \cos\phi \dfrac{\partial N_i}{\partial s} & \sin\phi \dfrac{\partial N_i}{\partial s} & 0 \\ \dfrac{N_i}{r} & 0 & 0 \\ 0 & 0 & -\dfrac{\partial N_i}{\partial s} \\ 0 & 0 & \dfrac{-N_i \cos\phi}{r} \\ -\sin\phi \dfrac{\partial N_i}{\partial s} & \cos\phi \dfrac{\partial N_i}{\partial s} & -N_i \end{bmatrix} \tag{A.1}$$

The derivative of this matrix with respect to the 2D, axisymmetrical element node radius r_i, $i = 1, 2$, see Fig. 8, is

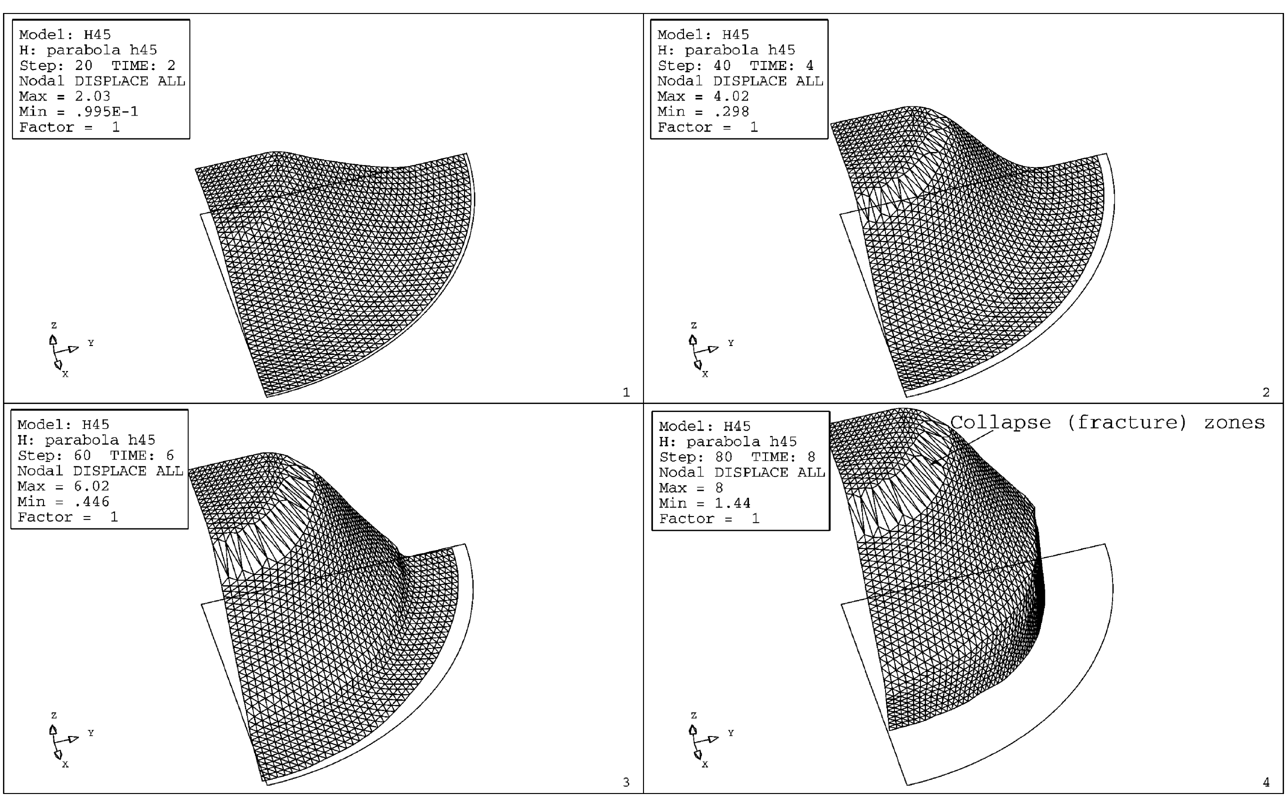

Fig. 8. HYDRAL test. Calculated deformed shapes for punch travels: (1) 2 mm; (2) 4 mm; (3) 6 mm; (4) 8 mm. Collapse (fracture) zones are indicated on fig, (4).

equal to

$$\frac{\partial \mathbf{B}_i}{\partial r_i} = \begin{bmatrix} -\sin\phi \frac{\partial N_i}{\partial s}\frac{d\phi}{dr} & \cos\phi \frac{\partial N_i}{\partial s}\frac{d\phi}{dr} & 0 \\ \frac{-N_i}{r^2} & 0 & 0 \\ 0 & 0 & 0 \\ 0 & 0 & \frac{N_i \sin\phi (d\phi/dr) r + N_i \cos\phi}{r^2} \\ -\cos\phi \frac{\partial N_i}{\partial s}\frac{d\phi}{dr} & -\sin\phi \frac{\partial N_i}{\partial s}\frac{d\phi}{dr} & 0 \end{bmatrix} \quad (A.2)$$

The derivative of elemental matrix $\mathbf{B}_i$ with respect to the coefficients of the parabola which passes through this element's nodes is much more complicated. Due to the complexity of analytical differentiation of the $\mathbf{B}_i$ matrix components with respect to the design parameters a system for doing mathematics by computer "Mathematica" [13] was used.

For 2-node linear element curvilinear coordinate s depends on natural (elemental) coordinate ξ as follows:

$$ds = \frac{l}{2} d\xi \quad (A.3)$$

The shape functions are equal to

$$N_1 = \frac{1-\xi}{2}, \qquad N_2 = \frac{1+\xi}{2} \quad (A.4)$$

where $-1 \le \xi \le 1$

After substitution of the last two equations into (A.1) we can obtain matrix $\mathbf{B}$ in the form

$$\mathbf{B}_i = \begin{bmatrix} \frac{(-1)^i}{l}\cos\phi & \frac{(-1)^i}{l}\sin\phi & 0 \\ \frac{1}{2\bar{r}} & 0 & 0 \\ 0 & 0 & \frac{-(-1)^i}{l} \\ 0 & 0 & \frac{-\cos\phi}{2\bar{r}} \\ \frac{(-1)^i}{l}(-\sin\phi) & \frac{(-1)^i}{l}\cos\phi & -\frac{1}{2} \end{bmatrix} \quad (A.5)$$

$$D[b11,a] = \frac{(y1+y2)\cos(2\arctan(1/b+ay1+ay2))}{(-y1+y2)(1+b^2+2aby1+a^2y1^2+2aby2+2a^2y1y2+a^2y2^2)} \quad (A.11)$$

$$D[b11,b] = \frac{\cos(2\arctan(1/b+ay1+ay2))}{(-y1+y2)(1+b^2+2aby1+a^2y1^2+2aby2+2a^2y1y2+a^2y2^2)} \quad (A.12)$$

Now $\mathbf{B}_i$ components depend on the radius of the center of the axisymmetrical, 1D shell element used in our finite element code:

$$\bar{r} = \tfrac{1}{2}(x_2 + x_1) \quad (A.6)$$

and on the angle between this element and horizontal coordinate axis, equals

$$\phi = \arctan\frac{(y_2 - y_1)}{(x_2 - x_1)} \quad (A.7)$$

The equation of parabola which lies on coordinate points 1 and 2 of those elements which are in full contact with parabolic part of the punch reads

$$x_1 = ay_1^2 + by_1 + c \quad (A.8)$$

$$x_2 = ay_2^2 + by_2 + c \quad (A.9)$$

"Mathematica" commands order for calculation of the derivative of the first component of matrix $\mathbf{B}_1$

$$b11 = \frac{-\cos[\phi]}{l} \quad (A.10)$$

is as follows:

$x1 = ay1^2 + by1 + c$
$x2 = ay2^2 + by2 + c$
$fi = \arctan[(y2 - y1)/(x2 - x1)]$
$l = (y2 - y1)/\sin[fi]$
$b11 = -\cos[fi]/l$
$D[b11, a]$
Simplify[
FortranForm[
TeXForm[

where D in "Mathematica" language denotes differentiation. Final result of this differentiation reads

$$D[b11, c] = 0 \quad (A.13)$$

All others components of matrix $\mathbf{B}_i$ can be differentiated in a similar way.

Matrix $\mathbf{B}$ of those elements which are not in full contact with parabolic part of the punch at specific time step does not depends directly on parabola parameters so we assume that its sensitivities with respect to parabola shape at this time step equals zero.

The determinant of the Jacobian matrix is given by formula

$$J = \sqrt{[J_1^2 + J_2^2]}$$

where

$$J_1 = \frac{1}{2}(x_2 - x_1)$$

and

$$J_2 = \frac{1}{2}(y_2 - y_1)$$

Gradients of this determinant with respect to the parabola coefficients for those elements which are in full contact with parabolic part of the punch can be again obtained by simple differentiation:

$$D[J,a] = \frac{(-y1 + y2)(b + ay1 + ay2)(-y1^2 + y2^2)}{4\sqrt{\frac{1}{4}(-y1+y2)^2 + \frac{1}{4}(-(by1) - ay1^2 + by2 + ay2^2)^2}} \tag{A.14}$$

$$D[J,b] = \frac{(-y1 + y2)^2(b + ay1 + ay2)}{4\sqrt{\frac{1}{4}(-y1+y2)^2 + \frac{1}{4}(-(by1) - ay1^2 + by2 + ay2^2)^2}} \tag{A.15}$$

$$D[J,c] = 0 \tag{A.16}$$

References

[1] K. Dems, Z. Mróz, Sensitivity analysis and optimal design of external boundaries and interfaces for heat conduction systems, J. Therm. Stresses 21 (1998) 451–488.

[2] M. Kleiber, H. Antunez, W. Sosnowski, Shape and non-shape sensitivity and optimization of metal forming processes, in: International Conference COMPLAS V, Computational Plasticity, Barcelona, 1997.

[3] M. Kleiber, H. Antunez, T.D. Hien, P. Kowalczyk, Parameter Sensitivity in Nonlinear Mechanics, Wiley, New York, 1997.

[4] M. Kleiber, T.D. Hien, H.J. Antunez, P. Kowalczyk, Parameter sensitivity of elasto-plastic response, Eng. Comput. 12 (1995) 263–280.

[5] M. Kleiber, W. Sosnowski, Parameter sensitivity analysis in frictional contact problems of sheet metal forming, Comput. Mech. 16 (1995).

[6] A. Mihelic, B. Stok, Tool design optimization in extrusion processes, Comput. Struct. 68 (1998) 283–293.

[7] E. Onate, C. Agelet de Saracibar, Numerical modeling of sheet metal forming problems, in: P. Hartley, et al. (Eds.), Numerical Modeling of Material Deformation Process, Springer, Berlin, 1992.

[8] K. Schittkowski, NLPQL: a fortran subroutine solving constrained nonlinear programming problems, Ann. Oper. Res. 5 (1986) 485–500.

[9] C.E.K. Silwa, E. Hinton, J. Sienz, L.E. Vaz, Structural shape optimization using elasto-plastic stress fields, in: Second World Congress of Structural and Multidisciplinary Optimization, IFTR PAS, Vol. 1, Zakopane, 1997, pp. 503–508.

[10] W. Sosnowski, M. Kleiber, A study on the influence of friction evolution on thickness changes in sheet metal forming, J. Mater. Proc. Technol. 1–4 (1996) 469–474.

[11] W. Sosnowski, E. Oñate, C. Agelet de Saracibar, Comparative study on sheet metal forming processes by numerical modeling and experiment, J. Mater. Proc. Technol. 34 (1992) 109–116.

[12] E.G. Thompson, R.D. Wood, O.C. Zienkiewicz, A. Samuelsson (Eds.), Numerical Methods in Industrial Forming Processes, Numiform'89, Balkena, 1989.

[13] S. Wolfram, Mathematica, A System for Doing Mathematics by Computer, Addison-Wesley, Reading, MA, 1991.

[14] O.C. Zienkiewicz, P.N. Godbole, Flow of plastic and viscoplastic solids with special reference to extrusion and forming processes, Int. J. Num. Meth. Eng. 8 (1979) 3–16.